Molecular Motion in Miscible Polymer Blends. 1. Motion in Blends of PEO and PVPh Studied by Solid-State ^{13}C $T_{1\rho}$ Measurements

Kevin S. Jack† and Andrew K. Whittaker*

Centre for Magnetic Resonance, University of Queensland, Queensland 4072, Australia

Received April 9, 1996; Revised Manuscript Received February 3, 1997⊗

ABSTRACT: Changes in molecular motion in blends of PEO−PVPh have been studied using measurements of ^{13}C $T_{1\rho}$ relaxation times. ^{13}C $T_{1\rho}$ relaxation has been confirmed as arising from spin−lattice interactions by observation of the variation in $T_{1\rho}$ with rf field strength and temperature. In the pure homopolymers a minimum in $T_{1\rho}$ is observed at ca. 50 K above the glass transition temperatures detected by DSC. After blending, the temperature of the minimum in $T_{1\rho}$ for PEO increased, while that for PVPh decreased, however, the minima, which correspond to the temperatures where the average correlation times for reorientation are close to 3.1 μs, are separated by 45 K (in a 45% PEO−PVPh blend). These phenomena are explained in terms of the local nature of $T_{1\rho}$ measurements. The motions of the individual homopolymer chains are only partially coupled in the blend. A short $T_{1\rho}$ has been observed for protonated aromatic carbons, and assigned to phenyl rings undergoing large-angle oscillatory motion. The effects of blending, and temperature, on the proportion of rings undergoing oscillatory motion are analyzed.

Introduction

Miscible polymer blends form a class of potentially attractive new materials since they provide a low-cost route to materials with properties which are a combination of those of the individual constituent polymers. For example, miscible blends have a single glass transition at temperatures intermediate to the glass temperatures of the component polymers. The blends therefore offer a simple route to tailoring mechanical properties of polymers. Recent work has shown that these so-called miscible blends are often in fact partially phase-separated at the very local scale, i.e. on the order of a few angstroms. This leads to the question of how the microphase separation affects the local motions of the individual polymer main-chains and side-chains, as these motions are sensitive to the details of the local packing of the polymer chains. These motions contribute to the glass transition, and to sub-T_g transitions such as the β-transition, and hence the mechanical properties of the blends. It is the aim of this paper to investigate the effect of blending on the local motions in a miscible polymer blend.

Poly(vinylphenol) (PVPh, Figure 1) has been shown to form miscible blends with a number of structurally-dissimilar polymers, e.g. poly(ethylene oxide) (PEO, Figure 1), poly(ϵ-caprolactone), poly(vinyl methyl ether) and poly(vinyl pyrrolidone).[1] Miscibility in all of these blends has been attributed to strong intermolecular hydrogen bonding between the hydroxy proton of PVPh and the oxygen-containing moiety, i.e. the carbonyl or ether, of the second polymer.[1,2] It has been reported[3] that blends of semicrystalline PEO with amorphous PVPh exhibit a single T_g over the entire composition range and that blends containing less than 50 wt % PEO are completely amorphous. Measurements of ^1H NMR relaxation times[4] have shown that the PVPh-rich blends are intimately mixed over distances less than 1−2 nm. The strong specific interaction between PEO and PVPh and the formation of a single amorphous phase in the PVPh-rich blends make these blends an ideal blend system for investigating the relationship between miscibility and molecular motion of the constituent polymers.

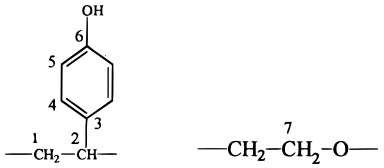

Figure 1. Structures of PVPh and PEO and the numbering scheme used in this work.

Molecular motion in blends of PEO−PVPh have been studied by measurements of ^1H T_2[4] and ^{13}C line widths.[5] Measurements of the ^{13}C line width of the meta-aromatic and the PEO carbons in two amorphous blends as a function of temperature demonstrated that the molecular motions of both PVPh and PEO are affected by blending but that the motions have a different characteristic temperature dependence. Measurements of ^1H T_2[4] in a blend containing 78 wt % PVPh showed that the PEO was restricted by the hard PVPh. A complex model of morphology was proposed to explain the ^1H T_2 results for the blend containing 58 wt % PVPh.

Methods for Studying Motion. In the past, molecular motion in polymer blends has been studied by a number of techniques, e.g. DMA, dielectric spectroscopy, and DSC. However, these techniques have generally only been capable of studying the bulk dynamic properties or the motion of only a single component of the blend. It has generally been accepted that in a miscible blend the low frequency, large amplitude, motion of both homopolymers would be concerted, i.e. have similar frequency distribution and amplitudes of motion, which are intermediate to those of the homopolymers. The detection of heterogeneity of motion by these techniques, for example as two glass transition temperatures, is therefore used as evidence for immiscibility of the homopolymers or morphological heterogeneity. The work presented here will demonstrate that blends classed as miscible by the aforementioned methods may

* Author to whom correspondence should be addressed.
† Current address: Department of Chemistry, Queen's University, Kingston, Ontario, K7L 3N6, Canada.
⊗ Abstract published in *Advance ACS Abstracts,* April 15, 1997.

S0024-9297(96)00535-9 CCC: $14.00

also display pronounced heterogeneity of chain motion as determined by NMR spectroscopy.

Heterogeneity of motion has previously been reported in miscible polymer blends using dielectric spectroscopy, and simultaneous IR dichroism and birefringence measurements.[6,7] Both of these techniques require, however, that the level of miscibility in the blends be determined by an alternative technique, e.g. ^{1}H NMR spectroscopy, although molecular level mixing in the blends can be inferred from changes in the motion of the homopolymers upon blending. Solid-state NMR spectroscopy has an advantage over other techniques for studying polymer blends, in that it can be used to determine not only the level of miscibility but also the motion of the individual homopolymers.[8−20]

Millar et al.[8] have used measurements of both ^{13}C and ^{1}H NMR line widths to study the miscibility and motion in blends of poly(vinylethylene)−1,4-poly(isoprene) (PVE−PI). ^{1}H NMR measurements demonstrated that the blends are miscible with domain sizes of less than 0.5−1.0 nm, while changes in ^{13}C line widths with temperature indicated that the motion of the two homopolymer chains had different temperature dependencies in the miscible blends. The authors concluded that the polymer chains in PVE−PI blends coexist in a single well-mixed phase but that the motions of the two homopolymers in the blends are not concerted.

Measurements of ^{13}C line width have also been reported for the miscible blends PVME−PSTY,[9,10] PEO−PVPh,[5] and PVPh−PMMA.[11] For these blends, the motion of the individual polymer chains was found to be affected by blending. However, the characteristic temperature dependencies of motion of the component polymers of the blends were shown to be different. It was concluded for all of these blends that the homopolymers must be interacting at a molecular level, yet the motion of the homopolymers was decoupled from each other to some extent.

The motion of PSTY and PVME in a 50% PSTY−PVME blend has been investigated using a heteronuclear correlation (or WISE) experiment.[12] At a temperature of 50 K above the glass transition detected by DSC, the ^{1}H spectrum of protons correlated with the PSTY carbons was broad, indicating that the frequency of motion of the PSTY was less than ca. 10 kHz, while the narrow line was due to PVME. This heterogeneity of motion could not be easily studied using 1D ^{1}H NMR spectroscopy.

Chung et al.[13,14] have use 2D ^{2}H exchange NMR to study the chain dynamics in miscible PVE−PI blends. The authors modeled the motion of the polymer chains using a log−Gaussian distribution of motional frequencies and by comparison of simulated and experimental spectra determined the mean mobility and width of the frequency distribution for each of the blends as a function of temperature. On blending, the two polymers had very different mean correlation times of motion, and the distribution of correlation times was broadened compared with those of the pure homopolymers. The broad DSC T_g was therefore ascribed to inherent differences in mobility of the two chains and to variations in composition throughout the blend. In a similar manner the work of Chin et al.[15,16] on PSTY−PPO blends, using 2D exchange NMR, ascribes heterogeneity of motion to local fluctuations in blend composition.

^{13}C Spin−Lattice Relaxation in Polymers. ^{13}C spin−lattice relaxation times in the rotating frame (^{13}C $T_{1\rho}$) have previously been shown to be sensitive to molecular motions in polymers with frequencies in the range of tens of kilohertz.[21−23] However, only one previous investigation of the motion of polymer blends using ^{13}C $T_{1\rho}$ measurements has been reported.[24] Simmons and Natansohn[24] have previously published an investigation of the molecular motion in a poly(donor)−poly(acceptor) blend. However, due to the large amount of overlap in the ^{13}C NMR spectrum of the homopolymers, an investigation of the motion of the main-chain and the side-chain of the homopolymers was not possible.

^{13}C $T_{1\rho}$ measurements provide many advantages for investigating molecular motion in polymer blends. The first of these advantages is that the ^{13}C $T_{1\rho}$ relaxation times are sensitive to molecular motions with frequencies of ca. 10−100 kHz (midkilohertz frequencies).[21] These frequencies are characteristic of the cooperative motions of polymer chains, that are liberated during the transition from the glassy to the rubbery state. Second, spin diffusion between ^{13}C nuclei is slow compared with ^{1}H spin diffusion, especially under conditions of MAS.[23] ^{13}C $T_{1\rho}$ relaxation times are not partially averaged by spin diffusion as are ^{1}H $T_{1\rho}$ relaxation times, and therefore information on the motion of each specific site is retained.

In contrast to this there are several factors which can complicate the interpretation of the observed relaxation times. First, it is not just the frequency of the molecular motion that determines the ^{13}C $T_{1\rho}$. The amplitude and anisotropy of the molecular motion will also affect the relaxation rate of the ^{13}C nuclei. Second, it has been long recognized that fluctuations of the dipolar field due to mutual ^{1}H−^{1}H spin flip-flops may also cause relaxation of the ^{13}C nuclei, in the absence of molecular motion.[21,25] This is the so called spin−spin relaxation process. Indeed the ^{13}C $T_{1\rho}$ relaxation time measured by spin-locking (^{13}C $T_{1\rho}$*) is the sum of two components:

$$1/^{13}\mathrm{C}\ T_{1\rho}^{*} = 1/^{13}\mathrm{C}\ T_{1\rho} + 1/T^{\mathrm{D}}_{\mathrm{CH}} \qquad (1)$$

These two components are the spin−lattice and the spin−spin relaxation processes with characteristic relaxation times of ^{13}C $T_{1\rho}$ and $T^{\mathrm{D}}_{\mathrm{CH}}$, respectively. The former processes are associated with motion of the ^{13}C−^{1}H bond vector with frequency components in the midkilohertz range. $T^{\mathrm{D}}_{\mathrm{CH}}$, however, is a function of the dipolar field strength and provides no information about motion. If the observed ^{13}C $T_{1\rho}$* is to be interpreted in terms of motion, then $T^{\mathrm{D}}_{\mathrm{CH}}$ must be much greater than ^{13}C $T_{1\rho}$; i.e. the spin−lattice processes dominate ^{13}C $T_{1\rho}$*.

An experimental procedure for determining the spin−lattice contribution to the ^{13}C $T_{1\rho}$* has been described by Stejskal et al.[26] and Schaefer et al.[27] This method requires the adiabatic alignment of protons in the dipolar field, which is difficult to implement on most commercial NMR spectrometers. In addition, the uncertainties associated with these measurements are also estimated to be large, ca. ±30%.[27] A semiqualitative method of calculating $T^{\mathrm{D}}_{\mathrm{CH}}$, based on measurements of the proton local field (H_L) and known values of $T^{\mathrm{D}}_{\mathrm{CH}}$ and H_L for a model polymer, has been proposed by Schaefer et al.[27]

Qualitative methods have also been suggested to test whether ^{13}C $T_{1\rho}$* is dominated by spin−lattice or spin−spin relaxation processes.[21] The most often used of these methods is the measurement of ^{13}C $T_{1\rho}$* as a function of the spin-locking field strength.[21,22,25,27−29] For relaxation dominated by the spin−lattice mechanism

^{13}C $T_{1\rho}$* will increase as the square of the rotating-frame field strength.[30] However, if ^{13}C $T_{1\rho}$* is dominated by spin−spin processes, then an exponential dependency of ^{13}C $T_{1\rho}$* on the rotating frame field is expected.[25] The range of field strengths which can be generated is typically only 30−70 kHz, and so it is often difficult, therefore, to provide conclusive evidence that a particular ^{13}C $T_{1\rho}$* is dominated by spin−lattice processes from the field dependency of ^{13}C $T_{1\rho}$* alone.

Finally, the observation of a minimum in ^{13}C $T_{1\rho}$ as a function of temperature is good evidence that relaxation is dominated by spin−lattice processes. If, on the other hand, ^{13}C $T_{1\rho}$ is dominated by spin−spin processes, it may be expected to decrease, but not increase, with increasing temperature as there is an increase in frequency and amplitude of motion which in turn modulates the dipole−dipole interactions.

There is a large body of evidence in the literature to show that ^{13}C $T_{1\rho}$ is dominated by spin−lattice processes in amorphous polymers in both the glassy and rubbery states. ^{13}C $T_{1\rho}$ and T^{D}_{CH} relaxation times have been determined experimentally for a number of glassy polymers including PSTY, PMMA, PPO,[26] poly(carbonate), poly(ethylene terephthalate),[22] and poly(α-methylstyrene).[27] In all cases it was concluded that the observed ^{13}C $T_{1\rho}$* relaxation was predominantly determined by spin−lattice processes and could be interpreted in terms of motion. Spin−lattice processes have also been shown to dominate the ^{13}C $T_{1\rho}$* in a cured DGEBA epoxy resin[31] and in poly(butyl acrylate)[32] over a broad range of temperatures. The spin−spin processes, generally, only become significant in determining the ^{13}C $T_{1\rho}$* of the crystalline regions in highly rigid and highly crystalline polymers, e.g. poly(oxymethylene),[26] poly(ethylene),[23,27] and poly(propylene).[28] Schaefer et al.[21,22] have concluded that in glassy polymers, the spin−lattice component is dominant and that the ^{13}C $T_{1\rho}$* is predominantly determined by motional processes, for spin-locking frequencies greater than ca. 30 kHz.

^{13}C $T_{1\rho}$* has also been shown to be sensitive to molecular motions in amorphous polymers above the T_g. Garroway et al.[23] have shown that the dominance of the ^{13}C $T_{1\rho}$* by spin−lattice processes extends on the high temperature side of the ^{13}C $T_{1\rho}$ minimum at sufficiently high spin-locking field strengths. Voelkel[32] has also shown that the ^{13}C $T_{1\rho}$* of poly(butyl acrylate) (T_g = −46 °C) is sensitive to motion both above and below T_g.

As it is evident that the observed ^{13}C $T_{1\rho}$* is predominantly determined by the spin−lattice relaxation processes in amorphous polymers close to the T_g, the * will be dropped when reporting ^{13}C $T_{1\rho}$ relaxation times in this paper. It will be confirmed below that spin−lattice processes dominate the ^{13}C $T_{1\rho}$ relaxation times of the blends studied in this work.

Aims. The aim of this paper is to demonstrate that measurements of ^{13}C $T_{1\rho}$ relaxation times can be used to study changes in molecular motion in miscible polymer blends. Changes in motion will be examined in blends of PVPh−PEO, which have previously been shown to be intimately mixed, in which there exists close molecular association induced by H-bonding. The relationship between the chain and side-group motion at 52 kHz and the glass transition temperature will be investigated. In addition the observation of biexponential ^{13}C $T_{1\rho}$ decays will be related to the proportion of phenyl rings in PVPh undergoing large-angle rapid oscillatory motion.

Table 1. Compositions, Glass Transition Temperatures and Crystallinity of PEO−PVPh Blends Used in This Study

blend composition (wt % PEO)	T_g (K)	crystallinity (% of total wt)	amorphous phase composition (wt % PEO)
PVPh	418	0	0
15% PEO	388	0	15
30% PEO	348	0	30
45% PEO	287	0	45
75% PEO	262	46.3	53.4
PEO	207	78.3	100

Experimental Section

The PEO sample was obtained from Janssen Chemical Co. and the PVPh sample from Polyscience Inc. and were kindly supplied by Dr. X. Zhang of Melbourne University. Both samples were used without further purification. The molecular weights of the two polymers have previously been determined to be M_w = 90 000 and 1500−7000 for PEO and PVPh, respectively. Blends of the polymers were prepared by casting of 0.5% w/v THF solutions into glass petri dishes, and drying at 60 °C for 5 days, followed by heating at 20 °C above the glass temperature for one day. Films were stored in a desiccant environment prior to examination.

The glass transition temperature (T_g) and crystallinity for PEO, PVPh, and each of the PEO−PVPh blends studied in this work were measured using a Perkin-Elmer DSC-7 using a heating rate of 20 °C/min. Temperatures were calibrated using indium and dodecane temperature standards, while the measurements of heat change were calibrated using an indium standard (ΔH_f = 28.45 J/g). The degree of crystallinity was calculated assuming an enthalpy of fusion for pure PEO crystals of 190 J g^{-1}.[33] Results are presented in Table 1. The compositions of the amorphous phase in each blend, calculated from the DSC data, are also shown in Table 1. As explained below, the NMR experiments detect only the amorphous phase in these blends; hence, the compositions quoted in the text are the compositions of the amorphous phase of each blend.

Solid-state ^{13}C CPMAS NMR spectra were recorded either on a MSL300 or a MSL200 spectrometer, operating at 75.46 and 50.38 MHz for ^{13}C, respectively. On the MSL300, samples were spun in a Bruker 7 mm DB MAS probe at spinning speeds of 3.1 kHz. On the MSL200 the samples were spun in a DOTY Scientific 7 mm MAS probe at 4.3 kHz. The $\pi/2$ pulse time on both spectrometers was 4.8 μs, corresponding to a spin-locking field strength of 52 kHz. ^{13}C $T_{1\rho}$ measurements were made by applying a ^{13}C spin-locking pulse after a 2 ms CP preparation period. The decay of the ^{13}C magnetization in the spin-locking field was followed for spin-locking times of up to 35 ms.

Results and Discussion

^{13}C NMR Spectra of PEO−PVPH Blends. The ^{13}C cross-polarization magic angle spinning (CPMAS) spectra of PVPh, PEO and the range of PEO−PVPh blends used in this investigation, are shown in Figure 2. The labels (1−7) on the spectra refer to the assignments of the seven peaks in the spectra to the structures shown in Figure 1 and are consistent with those reported by Zhang et al.[4] All other peaks in the ^{13}C NMR spectra are due to spinning side bands associated with the four aromatic resonances of PVPh, as was confirmed by measurement of the CPMAS spectrum of PVPh at a second MAS rate. The ^{13}C chemical shifts at 298 K for each of the seven carbon resonances in the spectra of the blends are given in Table 2.

From Table 2 it can be seen that only the hydroxyl carbon resonance of PVPh (peak 6) shows a systematic change in chemical shift with changing PEO content. The variation in chemical shift of this peak as a function of PEO composition is plotted in Figure 3. Qin et al.[3]

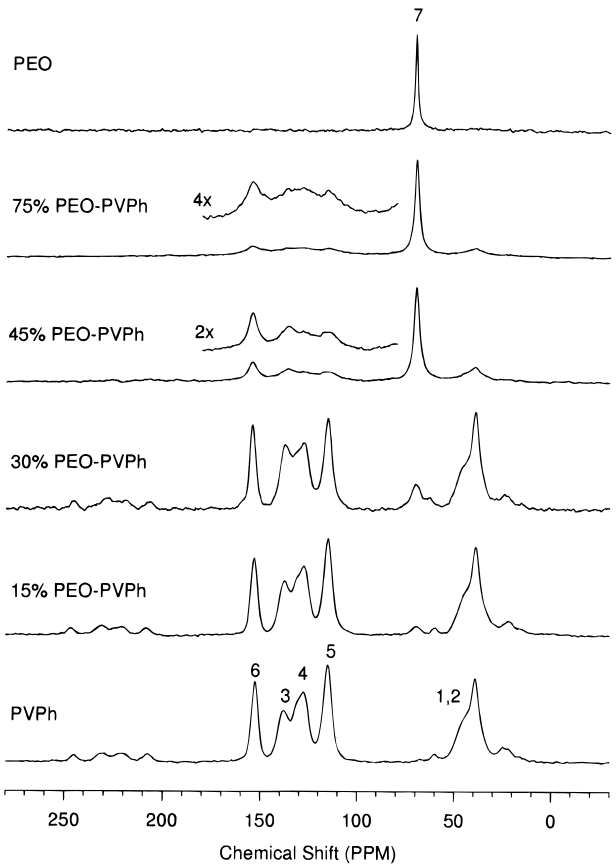

Figure 2. ^{13}C CPMAS spectra of PVPh, PEO, and blends of PEO−PVPh.

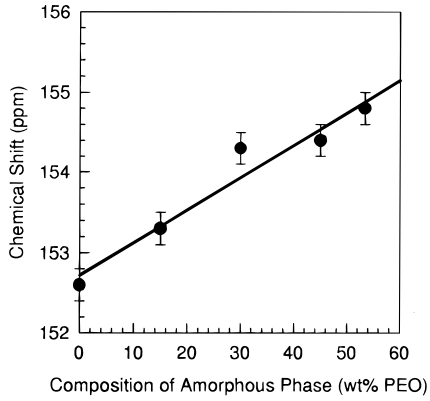

Figure 3. ^{13}C chemical shift of the peak due to carbon 6 of PVPh as a function of PEO content in the amorphous phase of PEO−PVPh blends.

Table 2. Chemical Shifts of the Peaks in the ^{13}C NMR Spectra of Blends of PEO−PVPh

	chemical shift of peaks (ppm)					
peak	PVPh	15% PEO	30% PEO	45% PEO	75% PEO	PEO
1,2	38.9	39.2	39.1	39.5	39.4	
3	138.1	137.9	137.8	135.9	136.3	
4	128.1	127.9	127.5	128.2	128.6	
5	115.2	115.4	115.2	115.7	116.0	
6	152.6	153.3	154.3	154.4	154.8	
7		69.5	70.2	70.6	69.8	70.3

and Zhang et al.[4] have also reported that the chemical shift of the hydroxyl resonance of PVPh shifts downfield by ca. 1−3 ppm upon addition of PEO. The decrease in the chemical shift of the quaternary aromatic peak of PVPh (peak 3), at PEO compositions greater than 30% PEO, is not considered significant, as this peak becomes very broad with increasing PEO composition and overlaps considerably with the peaks due to the ortho-aromatic carbons of PVPh (peak 4).

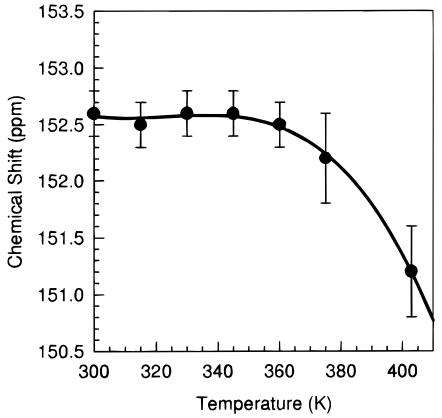

Figure 4. ^{13}C chemical shift of the peak due to carbon 6 of PVPh in PVPh homopolymer as a function of temperature.

Previously it has been shown that nonbonded interactions between the components of a polymer blend, e.g. charge-transfer interactions or hydrogen bonding, can result in changes in the ^{13}C chemical shifts of those carbons involved in the interaction, due to changes in the electron density surrounding these carbons.[34−38] Belfiore et al.[37] have shown that the hydroxyl resonance of resorcinol (1,3-dihydroxybenzene) is shifted downfield by ca. 3 ppm in blends with PEO due to hydrogen bonding. This result is in good agreement with the ca. 2 ppm downfield shift seen above for the hydroxyl resonance of PVPh. FTIR studies of PEO−PVPh blends have also shown that the relative proportion of hydrogen-bonded to non-hydrogen-bonded hydroxyl groups gradually increases as the PEO content is increased.[3] The approximately linear increase in the chemical shift of the hydroxyl peak of PVPh with increasing PEO content, shown in Figure 3, is, therefore, the result of an increase in the population of intermolecular hydrogen bonding between PVPh and PEO. Such behavior implies that molecular level mixing of PEO and PVPh occurs in these blends.

Qin et al.[3] have also reported that the phenol rings in pure PVPh can be in either a hydrogen-bonded (self-associated) or non-hydrogen-bonded state, based on FTIR and ^{13}C NMR results. In Figure 4 the ^{13}C chemical shift of the hydroxyl resonance of PVPh is plotted as a function of temperature. The chemical shift of this peak remains constant as the temperature is increased from 300 to ca. 370 K. However, when the temperature is increased beyond ca. 370 K, the chemical shift of the hydroxyl peak is shifted upfield. At 403 K an upfield shift of ca. 1.3 ppm is observed. This upfield shift is consistent with a reduction in the population of self-associated phenol groups, at temperatures greater than 370 K. As discussed below, an increase in the spectral density of motion of the phenyl rings of PVPh is detected by ^{13}C $T_{1\rho}$ measurements at these temperatures.

From Figure 2 we can see that as the PEO content of the blend increases, and the T_g therefore decreases, the line widths of the peaks in the ^{13}C CPMAS spectra due to PVPh increase markedly. This is due to an increase in the spectral density of midkilohertz frequency motions in the PEO−PVPh blends. It can be noted, for example that the line width of the aromatic peak at 152.9 ppm increases from 190 Hz in the 30% PEO blend to 400 Hz in the 53% PEO blend. It has previously been

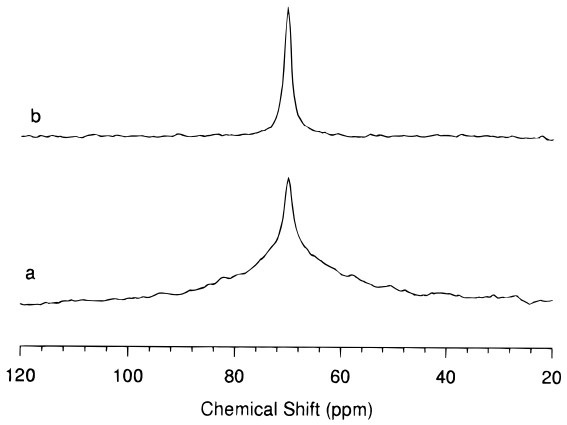

Figure 5. ^{13}C CPMAS spectra of PEO collected with cross-polarization contact times of 150 μs (a) and 2 ms (b).

demonstrated that the efficiency of dipolar decoupling is greatly reduced when the frequency of molecular motions is close to that of the decoupling field strength.[39,40] The contributions to the ^{13}C line widths in ^{13}C CPMAS spectra have been discussed and modeled by Takagoshi et al.[9] Importantly Takagoshi et al.[9] predict that as the mean frequency of motion increases beyond the midkilohertz frequency range the lines should commence to become narrow again. We do not observe a decrease in line width at the highest PEO contents, despite the T_g of the 53% PEO blend being 36 K below the measurement temperature.

Effect of Crystallinity on Spectra of PEO and Blends of PEO−PVPh. Figure 5 shows the ^{13}C CPMAS spectra of PEO collected with two different cross-polarization (CP) times (150 μs and 2 ms). The spectrum collected with a CP time of 150 μs is composed of overlapping narrow and broad resonances at ca. 70.4 ppm, which have been assigned to the methylene carbons of PEO in the amorphous phase and in the crystalline phase, respectively.[41−43] A small difference in the chemical shift, ca. 0.7 ppm, between the peaks due to amorphous and crystalline PEO has been reported; however, this is difficult to detect due to the breadth of the peak due to the crystalline component.[42,43] The CPMAS spectrum collected with a 2 ms CP time shows, however, only a single narrow resonance at 70.3 ppm, due to PEO in the amorphous region of the polymer.[41] The ^{13}C NMR signal from the PEO crystallites is eliminated in this experiment due to the rapid ^1H $T_{1\rho}$ relaxation of the protons in the crystalline region at room temperature (ca. 150 μs[41−43]). A CP time of 2 ms was therefore chosen for observation of the NMR signal from the amorphous phase only, in pure PEO and in blends containing a crystalline PEO phase.

Measurements of ^{13}C $T_{1\rho}$ Relaxation Times. ^{13}C $T_{1\rho}$ relaxation times were measured from the decay of magnetization during a ^{13}C spin-locking pulse after preparation of magnetization by cross-polarization. The decay curve measured for the meta-aromatic carbon 4 of the 30% PEO−PVPh blend, at 298 K, shown in Figure 6, is typical of all the relaxation curves obtained in this study.

^{13}C $T_{1\rho}$ relaxation times were determined from the ^{13}C $T_{1\rho}$ decay curves using a nonlinear least-squares (NLLS) fitting procedure. The "best" NLLS fit of a biexponential decay to the decay curve for carbon 5 is shown as a solid line in Figure 6. A single exponential decay was adequate for describing the relaxation behavior of the hydroxyl, unprotonated aromatic, PVPh

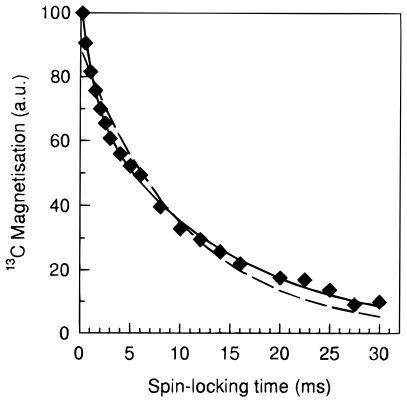

Figure 6. ^{13}C $T_{1\rho}$ decay curve for carbon 4 in 30% PEO−PVPh blend at 298 K. The lines are the result of fitting the curves to single (dashed line) and biexponential (solid line) decay processes.

Table 3. ^{13}C $T_{1\rho}$ for PVPh at 298 K as a Function of rf Field Strength

	^{13}C $T_{1\rho}$ (ms)		
rf field (kHz)	aromatic short ^{13}C $T_{1\rho}$	aromatic long ^{13}C $T_{1\rho}$	aliphatic carbons
40	2.8	51.7	33.7
52	2.1	60.1	64.1
69	4.7	81.8	92.0

aliphatic, and PEO carbons (carbons 6, 3, 1−2, and 7, respectively) in all experiments. However, the ^{13}C $T_{1\rho}$ decays of the protonated aromatic carbons of PVPh (carbons 4 and 5) were clearly best described by a biexponential decay. The result of fitting a single exponential to the data in Figure 6 is shown as a dashed line. Again this behavior was typical for all of the blend compositions measured, and at all measurement temperatures.

PVPh Homopolymer. In Table 3, the ^{13}C $T_{1\rho}$ relaxation times for the aromatic and aliphatic carbons of PVPh are reported as a function of rf field strength. As these measurements were collected at a ^{13}C resonance frequency of 75.4 MHz and a MAS rate of 3.1 kHz, there is extensive overlap between the isotropic peaks and spinning side bands, cf. the spectra reported in Figure 2, which were collected at 50.3 MHz and a MAS rate of 4.3 kHz. The ^{13}C $T_{1\rho}$ relaxation times are shown for the aromatic peaks were obtained from the decay of the intensity of the integrated region from 137.5−153.5 ppm and are an average of those for the four aromatic carbon resonances of PVPh (peaks 3−6). The ^{13}C $T_{1\rho}$ relaxation times for the aliphatic carbons were obtained from the long-time component of the decay of the region from 37−41 ppm. This region also contains significant intensity from spinning sidebands of the aromatic region of PVPh. Hence the ^{13}C $T_{1\rho}$ reported at 52 kHz is longer than that shown at the same field strength in Figure 6. The overlap between the spinning side bands and isotropic peaks in these experiments does not, however, affect the spin−lattice contribution to the ^{13}C $T_{1\rho}$ measured.

As discussed in the Introduction, if ^{13}C $T_{1\rho}$ is determined solely by spin−lattice processes, then ^{13}C $T_{1\rho}$ would be proportional to the square of the applied spin-locking field strength.[30] On the other hand, if ^{13}C $T_{1\rho}$ is determined solely by spin−spin processes then ^{13}C $T_{1\rho}$ would be expected to increase exponentially with increasing rf field strength.[31] Examples of measurements of the dependence of ^{13}C $T_{1\rho}$ on the rf field strength, in systems dominated by either spin−lattice

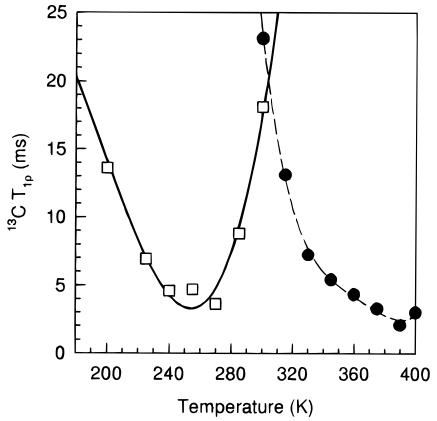

Figure 7. ^{13}C $T_{1\rho}$ of the peaks due to the aliphatic carbons of PVPh (●) and PEO (□) in the pure homopolymers, as a function of temperature.

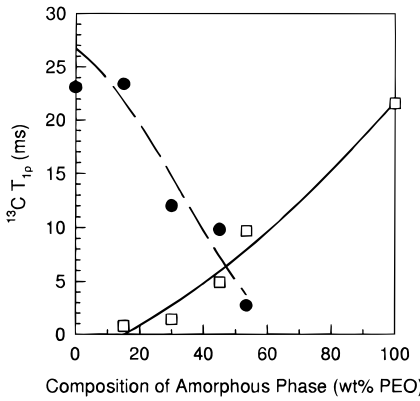

Figure 8. ^{13}C $T_{1\rho}$ of the peaks due to the aliphatic carbons of PVPh (●) and PEO (□) in PEO−PVPh blends at 298 K, as a function of blend composition.

or spin−spin mechanisms, can be found in the literature.[21,22,25,27−29] Clearly the ^{13}C $T_{1\rho}$ relaxation times in Table 3 are only weakly dependent on the rf field strength. It is therefore concluded that the ^{13}C $T_{1\rho}$ relaxation times for PVPh are determined by spin−lattice processes and can be interpreted in terms of motion. The spin−lattice contribution to the observed ^{13}C $T_{1\rho}$ has also been investigated in a number of glassy polymers which are structurally similar to PVPh, e.g. PSTY,[26] poly(*p*-bromostyrene), poly(*p*-chlorostyrene), and poly(*p*-methylstyrene).[29] For all of these polymers, ^{13}C $T_{1\rho}$ relaxation times are dominated by spin−lattice processes.

As a final verification that the ^{13}C $T_{1\rho}$ of PVPh is sensitive to the liberation of midkilohertz frequency motions in the region of the T_g, ^{13}C $T_{1\rho}$ values of the peak due to the aliphatic carbons of PVPh, as a function of temperature from 300−390 K, are shown in Figure 7. ^{13}C $T_{1\rho}$ decreases over this temperature range and is approaching a minimum at a temperature beyond the maximum temperature measured. It was not possible to measure ^{13}C $T_{1\rho}$ beyond the T_g of PVPh due to its low molecular weight and tendency to flow under the influence of MAS. Nonetheless it is clear from Figure 7 that the ^{13}C $T_{1\rho}$ of PVPh main-chain carbons decreases as the glass transition region is approached.

PEO Homopolymer. Previous measurements have shown that ^{13}C $T_{1\rho}$ of the crystalline region of semicrystalline polymers such as poly(oxymethylene),[26] poly(ethylene),[23,27] and poly(propylene)[28] are dominated by spin−spin processes. It has been concluded that spin−spin processes are important in determining the ^{13}C $T_{1\rho}$ in strongly dipolar-coupled systems such as semicrystalline polymers.[32] In contrast, this investigation is concerned with the motion of polymer chains in the amorphous regions of PEO and the blends of PEO−PVPh. VanderHart and Garroway[23] have shown that the ^{13}C $T_{1\rho}$ of amorphous polymers above T_g can be expected to be dominated by spin−lattice processes. For example, Voelkel[32] has shown that the ^{13}C $T_{1\rho}$ of poly(butyl acrylate) is sensitive to molecular motion above T_g. In the same manner as above, ^{13}C $T_{1\rho}$ measured at 298 K for both the crystalline and amorphous regions of PEO at different rf field strengths are reported in Table 4. The amorphous region of PEO shows a weak inverse relationship between ^{13}C $T_{1\rho}$ and the spin-locking field strength, while the ^{13}C $T_{1\rho}$ of the crystalline region is insensitive to variations in the rf field strength. From these results, it can be concluded that ^{13}C $T_{1\rho}$ is dominated by spin−lattice processes in both the amorphous and crystalline regions of PEO. Note that chains in the crystalline region of PEO undergo midkilohertz frequency motions at 298 K. Also as above, the ^{13}C $T_{1\rho}$ of the amorphous phase of PEO has been measured as a function of temperature (Figure 7). A minimum in the plot of ^{13}C $T_{1\rho}$ as a function of temperature, close to the T_g, is only expected if ^{13}C $T_{1\rho}$ is sensitive to molecular motion, i.e. dominated by spin−lattice processes. It is therefore concluded that the ^{13}C $T_{1\rho}$ relaxation times of the amorphous phase of PEO are due to spin−lattice processes and can be interpreted in terms of molecular motion. No attempt has been made to fit the variation in ^{13}C $T_{1\rho}$ as a function of temperature to an activated process and a distribution of correlation times, due to the possible minor contribution of the spin−spin mechanism at temperatures below the minimum in ^{13}C $T_{1\rho}$.

Table 4. ^{13}C $T_{1\rho}$ for PEO at 298 K as a Function of rf Field Strength

	^{13}C $T_{1\rho}$ (ms)	
rf field (kHz)	amorphous region	crystalline region
43	10.2	0.6
54	10.9	0.7
71	9.3	0.6
78	8.9	0.6

Motion of PVPh Chains in Blends of PEO−PVPh. In Figure 8, the ^{13}C $T_{1\rho}$ relaxation times of the overlapping aliphatic carbon peaks of PVPh (peaks 1,2 in Figure 2), measured at 298 K, are plotted as a function of the composition (wt % PEO) of the amorphous phase of the blend. As explained above, the ^{13}C $T_{1\rho}$ decays for the aliphatic carbons were well described by a single exponential decay. It can be seen from Figure 8 that the ^{13}C $T_{1\rho}$ of the PVPh aliphatic carbons decreases as the composition of PEO is increased, up to the maximum PEO content in the amorphous phase (53% PEO). This decrease results from an increase in the density of midkilohertz frequency motions of the PVPh as the glass transition temperature of the blend decreases toward the measurement temperature (298 K). Previous authors have shown that ^{13}C $T_{1\rho}$ in a glassy polymer decreases as the temperature is increased toward the T_g.[21,32] Voelkel[32] has demonstrated that ^{13}C $T_{1\rho}$ of poly(butyl acrylate) as a function of temperature shows a minimum at ca. 30 K above the T_g. The 30 K difference in the temperature of the ^{13}C $T_{1\rho}$ minimum and that of the T_g determined by DSC is due to the difference in the observation frequency of the two techniques. The former technique is sensitive to the onset of molecular motions at ca. 25 kHz (the rf field

strength used in Voekel's work was 25 kHz), while the latter is detecting the onset of molecular motion at ca. 0.1 Hz.

Qualitatively, a minimum in the plot of ^{13}C $T_{1\rho}$ vs composition of the blend (Figure 8) would be expected if the measurement temperature was above the T_g of a particular blend. This is the case for blends containing 45 and 53% PEO, which have T_g values determined by DSC of 287 and 262 K, respectively. The absence of a minimum in the Figure 8 suggests, however, that the motion of the PVPh is still restricted, i.e. glassy in nature, even in the 53% PEO−PVPh blend, where the observation temperature is ca. 40 K above the T_g of the blend.

Motion of PEO Chains in Blends of PEO−PVPh. Figure 8 also shows the ^{13}C $T_{1\rho}$ relaxation times at 298 K for the PEO chains in the amorphous regions of PEO−PVPh blends. The ^{13}C $T_{1\rho}$ values of the amorphous PEO decreases as the composition of PEO in the blends decreases, i.e. as the T_g of the blend increases. This behavior is the opposite of that observed for the aliphatic carbons of PVPh, as a function of blend composition.

The reduction in the ^{13}C $T_{1\rho}$ of the amorphous PEO at 298 K with increasing PVPh content implies that the addition of PVPh is effective in restricting the motion of the PEO chains. This is analogous to cooling PEO homopolymer from 300 K to ca. 255 K (Figure 7). However, as is shown in Figure 7, the ^{13}C $T_{1\rho}$ of amorphous PEO passes through a minimum at ca. 50 K above the T_g determined by DSC and increases at lower temperatures. It follows that a minimum in the plot of ^{13}C $T_{1\rho}$ vs composition is expected at ca. 53% PEO−PVPh, when the DSC-T_g of the blend is 40 K below room temperature.

The absence of a minimum in Figure 8 at a blend composition ≥45% PEO implies that the motion of PEO in the PEO−PVPh blends is less restricted than is expected on the basis of DSC measurements. In fact the absence of a minimum in the plot of ^{13}C $T_{1\rho}$ vs composition implies that the PEO chains are behaving as if they were above the T_g for all compositions measured. DSC measurements of the 15% PEO−PVPh blend, however, reveal that the T_g of this blend is ca. 90 K above room temperature (T_g = 388 K). The opposite behavior was observed for PVPh, in that the PVPh chains are more restricted than expected, on the basis of T_g measurements of the blends. Hence the motional states of the PEO and PVPh polymer chains in these miscible blends are clearly different. The motions of the component homopolymers in these blends are clearly affected by the intimate mixing that occurs in these blends but still remain independent of each other.

Comparison of Chain Motion in Blends of PEO−PVPh. Values of ^{13}C $T_{1\rho}$ for the nonprotonated aromatic carbons of PVPh and the methylene carbons of PEO in the 45% PEO−PVPh blend as a function of temperature from 255 to 345 K are presented in Figure 9. As the temperature is increased from 245 K the ^{13}C $T_{1\rho}$ relaxation times of the PEO carbons initially decrease, passing through a minimum at ca. 280 K, and then begin to increase. The ^{13}C $T_{1\rho}$ relaxation times of PVPh show a similar trend; however, the minimum in this curve occurs at ca. 325 K. Table 5 shows the temperatures of the ^{13}C $T_{1\rho}$ minima measured for both PEO and PVPh in the 45% PEO−PVPh blend and for the pure homopolymers.

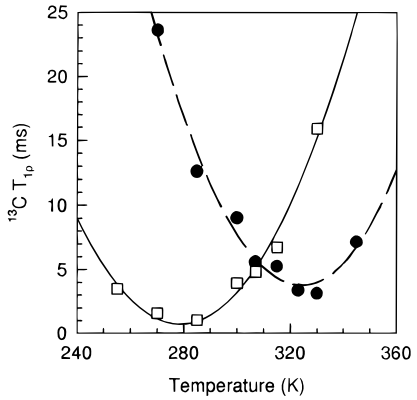

Figure 9. ^{13}C $T_{1\rho}$ of the peaks due to the aromatic carbons of PVPh (●) and aliphatic carbons of PEO (□) in a 45% PEO−PVPh blend, as a function of temperature.

Table 5. Temperatures of the Minima of ^{13}C $T_{1\rho}$ for PEO and PVPh in Blend and Homopolymers

	temp (K)	
	pure homopolymer	45% PEO−PVPh
amorphous PEO	255	280
PVPh	>360	325

As all of these experiments were obtained using the same spin-locking field strength ($\omega_1 = 3.3 \times 10^5$ rad/s), then each of the minima shown in Table 5 occur when the polymer chains have the same average τ_c ($\tau_c = 3.1$ μs). Blending of PEO and PVPh shifts the temperature at which $\tau_c = 3.1$ μs for each of the homopolymers. In the case of PEO, the temperature of the ^{13}C $T_{1\rho}$ minimum is increased by 25 K, which implies that the motion of the PEO chains is restricted by the intimate mixing with PVPh. The ^{13}C $T_{1\rho}$ minimum for PVPh is, however, decreased by >35 K, which is consistent with an increase in the frequency of molecular motions of the PVPh chains at any given temperature on blending. The difference in the ^{13}C $T_{1\rho}$ minima of PEO and PVPh in the 45% PEO−PVPh blend implies that the distribution of motional frequencies is different for the two homopolymers; i.e., the average τ_c of the homopolymers is different.

As discussed above, the 45% PEO−PVPh blend has a single T_g detected by DSC at 287 K. The fact that two separate minima are observed in the plots of ^{13}C $T_{1\rho}$ vs temperature, both of which are different from the DSC T_g, is best explained in terms of the spatial sensitivity of the two techniques. The ^{13}C NMR technique is sensitive to fluctuating dipolar fields caused predominantly by the motions of C−H dipoles within a few bonds of an isolated ^{13}C nuclei, i.e. on the order of ca. 0.1−0.4 nm. DSC, however, is thought to be sensitive to motions over a scale of hundreds of bonds. Work by Kaplan[44] would suggest that DSC and DMA provides dynamic information that is averaged over a distance of ca. 20−100 nm. PEO−PVPh blends have been shown by ^1H $T_{1\rho}$ measurements to be homogeneous over much smaller sizes (<2−3 nm),[4] and therefore an average T_g would be observed by DSC. A broadening of the T_g transition observed in the DSC of these blends, and which is often reported in the DSC of miscible polymer blends, is due partly to the differences in chain dynamics of the component homopolymers, detected by the ^{13}C $T_{1\rho}$ technique.

Motion of Phenyl Rings in PVPh. The ^{13}C $T_{1\rho}$ decay curves of the protonated aromatic carbons of PVPh (peaks 4 and 5), unlike those for the other carbon

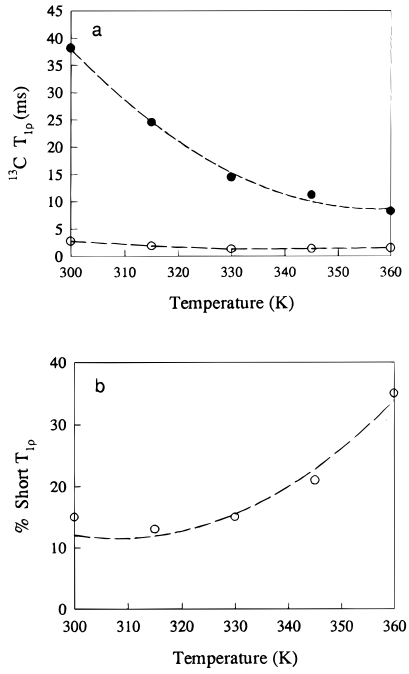

Figure 10. Short and long ^{13}C $T_{1\rho}$ values for the peak due to the meta-aromatic carbons of PVPh in PVPh homopolymer, as a function of temperature (a), and percentage of short ^{13}C $T_{1\rho}$ (b) determined by NLLS analysis.

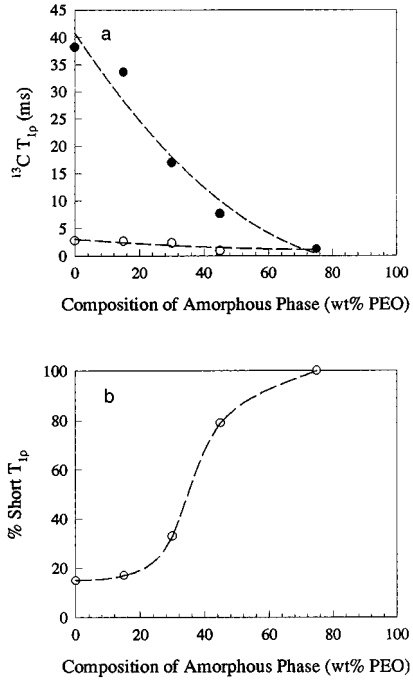

Figure 11. Short and long ^{13}C $T_{1\rho}$ values for the peak due to the meta-aromatic carbons of PVPh in PEO−PVPh blends, as a function of the composition of the blend (a), and percentage of short ^{13}C $T_{1\rho}$ (b) determined by NLLS analysis.

resonances, could not be adequately described by a single exponential decay process, and instead for these carbons the decay curves were fitted to a biexponential decay, as shown in Figure 6. A biexponential decay function was chosen for simplicity and was chosen because important insights into the nature of the motion of the phenyl rings can be gained from the changes in the decay curves. The values and proportions of the short and long ^{13}C $T_{1\rho}$ for the meta-aromatic carbons (peak 5 in Figure 2) as a function of temperature in pure PVPh are presented in Figure 10. Figure 11 shows the ^{13}C $T_{1\rho}$ data for this same peak as a function of blend composition. The trends in both the relaxation times and the relative contribution of the short and long components to the ^{13}C $T_{1\rho}$ decays for the ortho-aromatic carbons, as a function of temperature and blend composition, are the same as for the meta-aromatic carbons and are not shown.

The decrease in the long $T_{1\rho}$ as a function of increasing temperature in PVPh homopolymer, or PEO content in the blend, is similar to the decrease in $T_{1\rho}$ of the aliphatic main-chain carbons shown in Figures 7−9. On the basis of this similarity the long $T_{1\rho}$ of the protonated aromatic carbons is assigned to phenol groups which are undergoing midkilohertz frequency motions associated with the glass transition phenomenon.

The short ^{13}C $T_{1\rho}$ for the protonated aromatic carbons of PVPh is assigned to phenol groups which are also experiencing large-angle oscillatory motion about the C_2 axis of the phenol group. This assignment is consistent with many experimental observations and previous assignments in the literature. For example, measurements at different rf field strengths have demonstrated that the short $T_{1\rho}$ is not due to spin−spin processes and therefore must be due to molecular motions with a frequency component in the midkilohertz region. We have observed small changes in the amplitude of the first positive and negative spinning side bands during the $T_{1\rho}$ experiment, which are consistent with oscillatory motion, but not full 180° ring flips.

In addition, from Figure 11 it can be seen that the relative number of phenol groups which contribute to the short $T_{1\rho}$ increases with increasing temperature. This increase is attributed to the increase in local free volume surrounding the phenol group. In Figure 11 it is noticeable that a more rapid increase in the population of rings which undergo the oscillatory motion occurs at ca. 345 K. This temperature is close to the temperature at which the chemical shift of the hydroxyl carbon (carbon 6, Figure 1) is observed to decrease in Figure 4. It was proposed above that this upfield shift is due to a decrease in hydrogen bonding. Oscillatory motion would result in a decrease in the H bonding of the hydroxyl protons.

Only the ^{13}C $T_{1\rho}$ decay curves for the protonated aromatic carbons of the phenol groups are described by a biexponential relaxation process. This is due to the relationship between the axis of rotation, for the oscillatory motion, and the ^{13}C−^{1}H dipolar vectors for each of the carbons on the phenol ring. The oscillatory motion is less effective in averaging the ^{13}C−^{1}H dipolar interactions associated with carbons 3 and 6, since the interactions are weaker and involve a larger number of long range intra-ring couplings to protons. On the other hand the dipolar interactions associated with the protonated aromatic carbons are dominated by well-defined coupling to the directly-bonded protons, which is more strongly modulated by the oscillatory motion. Hence, this type of motion only provides an effective spin−lattice relaxation pathway for the protonated aromatic carbons, provided the frequency of this motion is in the midkilohertz region.

Poliks et al.[45] have measured $\langle^{13}$C $T_{1\rho}\rangle$ relaxation times for the protonated aromatic carbon resonances of poly(ether ether ketone) (PEEK), as a function of the polymer crystallinity. $\langle^{13}$C $T_{1\rho}\rangle$ is defined as the ^{13}C $T_{1\rho}$ determined from the decay of the ^{13}C magnetization during the first 1 ms of the spin-locking experiment; i.e. it is similar to the short $T_{1\rho}$ reported here. The authors have shown that $\langle^{13}$C $T_{1\rho}\rangle$ decreases as the crystallinity

of the PEEK decreases, reflecting an increase in the population of phenyl groups undergoing the ring-flipping motion. Similar results have been presented by Schaefer et al.[29] in their study of the motion of the phenyl ring in PSTY. In this latter work $\langle^{13}C\ T_{1\rho}\rangle$ of the flipping phenyl groups is on the order of 7 ms.[29]

From Figure 10 it can be seen that the value of short $T_{1\rho}$ changes little across the temperature range 300−390 K. This insensitivity to changes in temperature suggests that the frequency distribution of the oscillatory motions is very broad and that variations in temperature do not significantly alter the spectral density of motions at ca. 52 kHz. Previous ^2H NMR investigations of phenyl group motion in PSTY have shown that the distribution of motional frequencies is very broad and extends over many decades.[46]

Motion of Phenyl Rings in Blends. We finally consider the motion of phenol rings in blends of PEO−PVPh When the composition of the blend is increased beyond 30% PEO, there is a rapid increase in the population of phenol groups undergoing oscillatory motion at 298 K (Figure 11). In the 45% PEO−PVPh blend, 78% of the phenol groups of PVPh contribute to the short $T_{1\rho}$. The value of the short $T_{1\rho}$ in the 45% PEO−PVPh is also observed to decrease, due to the large increase in the spectral density of oscillatory motions in the midkilohertz frequencies. At higher PEO compositions a single ^{13}C $T_{1\rho}$ is observed since the majority of the phenyl rings are undergoing oscillatory motions and the long $T_{1\rho}$ has decreased to be indistinguishable from the short $T_{1\rho}$. This increase in phenol ring mobility is attributed to an increase in local free volume around the phenol groups, due to the decrease in T_g of the blends with increasing PEO content.

Conclusions

Measurements of ^{13}C $T_{1\rho}$ have been shown to be a sensitive probe of changes in molecular motion occurring in miscible polymer blends. Information on the motion of both the side- and main-chain can be obtained rapidly. Measurements as a function of temperature and rf field strength have confirmed that the relaxation is indeed due to motional processes.

In the miscible blend PEO−PVPh, the motions of the two homopolymers are affected by the blending, with decreases and increases in the frequency of motion for PEO and PVPh, respectively, compared with the motion in the homopolymers at the same temperature. However, differences in the temperatures of the minima of ^{13}C $T_{1\rho}$ were observed for the two polymers in the blend. Thus the frequency of motion of the main chains in the 45% PEO−PVPh blend differ by several orders of magnitude at ambient temperatures. It is concluded that the motions of the polymers in this miscible blend are only weakly coupled.

An additional short ^{13}C $T_{1\rho}$ process was observed for protonated carbons in phenyl groups. This was assigned to rings undergoing large-angle oscillatory motion. The proportion of rings in PVPh undergoing this motion increases on increases in temperature or on blending with PEO.

References and Notes

(1) Moskala, E. J.; Varnell, D. F.; Coleman, M. M. *Polymer* **1985**, *25*, 228.
(2) Le Menetrel, C.; Bhagwagar, D. E.; Painter, P. C.; Coleman, M. M. *Macromolecules* **1992**, *25*, 7101.
(3) Qin, C.; Pires, A. T. N.; Belfiore, *L. A. Polym. Commun.* **1990**, *31*, 177.
(4) Zhang, X.; Takegoshi, K.; Hikichi, K. *Macromolecules* **1992**, *25*, 2336.
(5) Zhang, X.; Takegoshi, K.; Hikichi, K. *Macromolecules* **1993**, *26*, 2198.
(6) Roland, C. M.; Ngai, K. L. *Macromolecules* **1992**, *25*, 363.
(7) Zawada, J. A.; Ylitalo, C. M.; Fuller, G. G.; Colby, R. H.; Long, T. E. *Macromolecules* **1992**, *25*, 2896.
(8) Miller, J. B.; McGrath, K. J.; Roland, C. M.; Trask, C. A.; Garroway, A. N. *Macromolecules* **1990**, *23*, 4543.
(9) Takegoshi, K.; Hikichi, K. *J. Chem. Phys.* **1991**, *94*, 3200.
(10) Le Menetrel, C.; Kenwright, A. M.; Sergot, P.; Laupretre, F.; Monnerie, L. *Macromolecules* **1992**, *25*, 3020.
(11) Zhang, X.; Takegoshi, K.; Hikichi, K. *Macromolecules* **1991**, *24*, 5756.
(12) Schmidt-Rohr, K.; Clauss, J.; Spiess, H. W. *Macromolocules* **1992**, *25*, 3273.
(13) Chung, G.-C. Kornfield, J. A.; Smith, S. D. *Macromolecules* **1994**, *27*, 964.
(14) Chung, G.-C.; Kornfield, J. A.; Smith, S. D. *Macromolecules* **1994**, *27*, 5729.
(15) Chin, Y. H.; Zhang, C.; Wang, P.; Jones, A. A.; Inglefield, P. T.; Kambour, R. T.; Bendler, J. T.; White, D. M. *Macromolecules* **1991**, *24*, 3031.
(16) Chin, Y.; Inglefield, P. T.; Jones, A. A. *Macromolecules* **1993**, *26*, 5372.
(17) Kwei, T. K.; Nishi, T.; Roberts, R. F. *Macromolecules* **1974**, *7*, 667.
(18) Douglas, D. C.; McBrierty, V. J. *Macromolecules* **1978**, *11*, 766.
(19) Caravatti, P.; Neuenschwander, P.; Ernst, R. R. *Macromolecules* **1986**, *19*, 1889.
(20) Chu, C. W.; Dickinson, L. C.; Chien, J. C. W. *J. Appl. Polym. Sci.* **1990**, *41*, 2311.
(21) Schaefer, J.; Stejskal, E. O.; Buchdahl, R. *Macromolecules* **1977**, *10*, 384.
(22) Schaefer, J.; Stejskal, E. O.; Steger, T. R.; Sefcik, M. D.; McKay, R. A. *Macromolecules* **1980**, *13*, 1121.
(23) VanderHart, D. L.; Garroway, A. N. *J. Chem. Phys.* **1979**, *71*, 2773.
(24) Simmons, A. Natansohn, A. *Macromolecules* **1992**, *25*, 3881.
(25) Garroway, A. N.; Moniz, W. B.; Resing, H. A. *ACS Symp. Ser.* **1979**, *103*, 67.
(26) Stejskal, E. O.; Schaefer, J.; Steger, T. R. *Faraday Soc. Symp.* **1979**, *13*, 56.
(27) Schaefer, J.; Sefcik, M. D.; Stejskal, E. O.; McKay, R. A. *Macromolecules* **1984**, *17*, 1118.
(28) Fleming, W. W.; Lyerla, J. R.; Yannoni, C. S. *ACS Symp. Ser.* **1984**, *247*, 83.
(29) Schaefer, J.; Sefick, M. D.; Stejskal, E. O.; McKay, R. A.; Dixon, W. T.; Cais, R. E. *Macromolecules* **1984**, *17*, 1107.
(30) Bloembergen, N.; Purcell, E. M.; Pound, R. V. *Phys. Rev.* **1948**, *73*, 679.
(31) Garroway, A. N.; Moinz, W. B.; Resing, H. A. *Faraday Soc. Symp.* **1979**, *13*, 63.
(32) Voelkel, R. *Angew. Chem., Int. Ed. Engl.* **1988**, *27*, 1468.
(33) Marco, C.; Fatou, J. G.; Gomez, M. A.; Tanaka, H.; Tonelli, A. E. *Macromolecules* **1990**, *23*, 2183.
(34) Natansohn, A.; Bazuin, C. G.; Tong, X. *Can. J. Chem.* **1992**, *70*, 2900.
(35) Simmons, A.; Natansohn, A. *Macromolecules* **1991**, *24*, 3651.
(36) Natansohn, A.; Simmons, A. *Macromolecules* **1989**, *22*, 4426.
(37) Belfiore, L. A.; Lutz, T. J.; Cheng, C.; Bronnimann, C. E. *J. Polym. Sci., Polym. Phys. Ed.* **1990**, *28*, 1261.
(38) Patwardhan, A.; Belfoire, L. A. *Polym. Eng. Sci.* **1988**, *28*, 916.
(39) Rothwell, W. P.; Waugh, J. S. *J. Chem. Phys.* **1981**, *74*, 2721.
(40) VanderHart, D. L.; Earl, W. L.; Garroway, A. N. *J. Magn. Reson.* **1981**, *44*, 361.
(41) Wobst, M. *J. Polym. Sci., Polym. Phys. Ed.* **1988**, *26*, 527.
(42) Dechter, J. J. *J. Polym. Sci., Polym. Lett. Ed.* **1985**, *23*, 261.
(43) Johansson, A.; Tegenfeldt, J. *Macromolecules* **1992**, *25*, 4712.
(44) Kaplan, D. S. *J. Appl. Polym. Sci.* **1976**, *20*, 2615.
(45) Poliks, M. D.; Schaefer, J. *Macromolecules* **1990**, *23*, 3246.
(46) Kulik, A. S.; Prins, K. O. *Polymer* **1993**, *34*, 463.

MA9605356